Velocity-independent Marchenko method in time- and depth-imaging domains

Yanadet Sripanich [1], *Ivan Vasconcelos* [1], *Kees Wapenaar* [2], *and Jeannot Trampert* [1]
[1] *Utrecht University*
[2] *Delft University of Technology*

SUMMARY

The Marchenko method represents a constructive technique to obtain Green's functions between the acquisition surface and any arbitrary point in the medium. The process generally involves solving an inversion starting with a direct-wave Green's function from the desired subsurface position, which is typically obtained using an approximate velocity model. In this study, we first propose to formulate the Marchenko method in the time-imaging domain. We recognize that the traveltime of the direct-wave Green's function is related to the Cheop's traveltime pyramid commonly used in time-domain processing and can be readily obtained from the local slopes of the common-midpoint (CMP) gathers. This observation allows us to substitute the need for a prior velocity model with the data-driven slope estimation process. Moreover, we show that working in the time-imaging domain allows for the specification of the desired subsurface position in terms of vertical time, which is connected to the Cartesian depth position via the time-to-depth conversion. Our results suggest that the prior velocity model is only required when specifying the position in depth but this requirement can be circumvented by making use of the time-imaging domain and its usual assumptions. Provided that those assumptions are satisfied, the estimated Green's functions from the proposed method have comparable quality to those obtained with the knowledge of a prior velocity model.

INTRODUCTION

Green's functions between the surface and any subsurface point serve as the main ingredient in seismic redatuming and imaging. The Marchenko method provides a constructive framework to obtain such information using the reflection data at the surface and an estimate of the direct-wave Green's function from the desired subsurface position (Broggini and Snieder, 2012; Broggini et al., 2012; Slob et al., 2014; Wapenaar et al., 2014b, 2017). Given a prior approximate (smooth) velocity model of the subsurface in Cartesian coordinates, one can specify the subsurface position and obtain the direct-wave Green's function from this position to the surface using a simple forward extrapolation (Wapenaar et al., 2014b; Thorbecke et al., 2017). An alternative strategy involves a separate inversion for the direct-wave Green's function from the common focal point (CFP) technology based on the same starting velocity model (Berkhout, 1997; Thorbecke, 1997). Therefore, a caveat to the current Marchenko method and its implementation is the requirement for prior velocity knowledge.

Conventional seismic imaging is accomplished in either time or depth domain. The former generally performs with higher computational efficiency, but becomes less accurate than the latter when dealing with geologically complex areas such as subsalt regions (Yilmaz, 2001). The shortcomings of time-imaging methods are largely due to the following (Fomel, 2013, 2014):

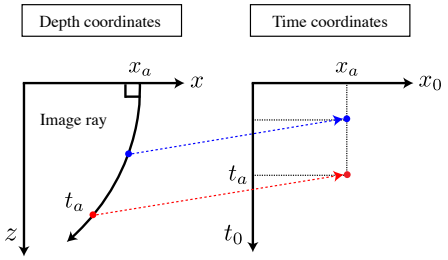

Figure 1: The relationship between depth- and time-imaging coordinates. An example image ray originating from x_a with orthogonal slowness vector to the surface is shown. Every point along this ray is mapped to the same lateral distance in the time domain with different traveltime t_a.

1. Approximate direct-wave Green's functions are used for imaging, which typically depend on hyperbolic or slightly non-hyperbolic traveltime approximations.
2. Each time-domain image point is associated with its own approximate effective velocity under the assumption of straight-ray geometry relative to the surface.
3. When lateral heterogeneity is present, the final images are generated in distorted coordinates defined by image rays (Hubral, 1977) as shown in Figure 1.

However, in view of areas with moderately complex geology where such assumptions are approximately valid, we can turn these limitations into our advantages. In particular, recent research on time-domain imaging has led to an alternative data-driven time-imaging workflow for improved efficiency and accuracy with local event slopes from CMP gathers instead of velocity (Fomel, 2007). This development leads to an opportunity to bring in a velocity-independent data-driven technique from time-domain imaging to estimate the direct-wave Green's functions and contribute to the Marchenko method.

In this paper, we first study the Marchenko method in the time-imaging domain and establish relationships between the focusing functions obtained from the Marchenko methods in both time- and depth-imaging domains. Making use of the slope-based time-domain processing workflow, we subsequently propose a scheme to obtain the direct-wave Green's function from the desired subsurface position on a reflector to the surface. We show by numerical examples that the newly estimated direct-wave Green's function can be used in the Marchenko method and leads to comparable results to those that rely on the prior knowledge of a velocity model.

MARCHENKO METHOD IN TIME-IMAGING DOMAIN

Reciprocity theorems with curvilinear datum levels

The key component to deriving the Marchenko equations is the one-way reciprocity theorems of both convolution and correlation types (Wapenaar and Grimbergen, 1996; Wapenaar et al., 2014a; van der Neut et al., 2015). Assuming that the image rays are well-defined with no caustics, we first recognize that a constant depth level in the Cartesian coordinates generally corresponds to a curved level in the time-imaging domain and vice versa. In other words, the current Marchenko method has already been implemented with respect to a curved level in the time-imaging domain. To show that a converse relationship exists, we need to find the Marchenko equations for a curvilinear level in depth that corresponds to a constant time surface.

Because the time-imaging domain is defined by image rays, it represents a special curvilinear coordinate system of semi-orthogonal type (Sava and Fomel, 2005) due to the orthogonality between the ray direction and the wavefront. The one-way reciprocity theorems for such curvilinear systems (ξ_1, ξ_2, ξ_3) = ($\boldsymbol{\xi}$, ξ_3) are given by (Frijlink and Wapenaar, 2010):

$$\int_{S_a} \left(p_A^+ p_B^- - p_A^- p_B^+\right) d\boldsymbol{\xi} = \int_{S_f} \left(p_A^+ p_B^- - p_A^- p_B^+\right) d\boldsymbol{\xi} \ , \quad (1)$$

$$\int_{S_a} \left(p_A^+ p_B^{+*} - p_A^- p_B^{-*}\right) d\boldsymbol{\xi} = \int_{S_f} \left(p_A^+ p_B^{+*} - p_A^- p_B^{-*}\right) d\boldsymbol{\xi} \ , \quad (2)$$

where equations 1 and 2 represent the one-way reciprocity theorems of convolution and correlation types, respectively. Here, p denotes the flux-normalized wavefields in the frequency domain decomposed into *upgoing* ($-$) and *downgoing* ($+$) constituents with respect to ξ_3 at S_a and S_f. The superscript $*$ denotes complex conjugation. The integrations are done at every point $\boldsymbol{\xi}$ over the acquisition surface S_a and the focusing surface S_f. Both of which no longer need to represent constant-depth surfaces. Similarly to the current derivation of the Marchenko method, the subscripts A and B denote the two acoustic states — the truncated medium and the true medium. Moreover, the considered region between S_a and S_f is assumed to have similar medium parameters and is source-free.

Marchenko equations in image-ray coordinates

We can clearly observe that equations 1 and 2 are similar to the one-way reciprocity theorems for the case of flat datum levels except that the integrations are now done over curvilinear surfaces. Therefore, we can follow a similar procedure as in the previous works and derive the Marchenko equations (Wapenaar et al., 2014a,b; van der Neut et al., 2015). This leads to the following system of equations in the frequency domain:

$$g^-(\boldsymbol{\xi}_f, \boldsymbol{\xi}_a) = \int_{S_a} R(\boldsymbol{\xi}'_a, \boldsymbol{\xi}_a) f_1^+(\boldsymbol{\xi}'_a, \boldsymbol{\xi}_f) d\boldsymbol{\xi}'_a - f_1^-(\boldsymbol{\xi}_a, \boldsymbol{\xi}_f) \ ,$$

$$-g^{+*}(\boldsymbol{\xi}_f, \boldsymbol{\xi}_a) = \int_{S_a} R^*(\boldsymbol{\xi}'_a, \boldsymbol{\xi}_a) f_1^-(\boldsymbol{\xi}'_a, \boldsymbol{\xi}_f) d\boldsymbol{\xi}'_a - f_1^+(\boldsymbol{\xi}_a, \boldsymbol{\xi}_f) \ , \quad (3)$$

which is similar to the original Marchenko system except for the integration over the curvilinear boundary S_a. $g^\pm$ denote the Green's functions and $f_1^\pm$ are the focusing functions defined in the truncated medium with a curved boundary. The variables $\boldsymbol{\xi}_a$ and $\boldsymbol{\xi}'_a$ are defined on the surface S_a, whereas $\boldsymbol{\xi}_f$ is defined at the focusing level S_f. Assuming that the acquisition surface S_a is flat, we have $\boldsymbol{\xi}_a = \mathbf{x}_a = (x, y)$ and the reflection response R can be expressed as (Wapenaar et al., 2014b):

$$R(\mathbf{x}'_a, \mathbf{x}_a) = \frac{2\partial_z \, g^-(\mathbf{x}'_a, \mathbf{x}_a)}{j\omega\rho(\mathbf{x}_a)} \ , \quad (4)$$

which is twice the pressure recording at $\mathbf{x}'_a$ from a vertical dipole source at $\mathbf{x}_a$.

Since equation 3 is similar to that in the case of a constant-depth focusing level, we can argue that the form of the Marchenko system remains the same as long as there exists a transformation between the Cartesian coordinates and some semi-orthogonal curvilinear coordinates, whose level curve matches with the desired curvilinear datum level. In the case of the time-imaging domain, the coordinate transformation is defined by the mapping of image rays for the time-to-depth conversion (Cameron et al., 2007; Sripanich and Fomel, 2018). In this paper, we define the image-ray coordinates as $\xi_1 = x_0$, $\xi_2 = y_0$, and $\xi_3 = t_0$ (Figure 1). The first two coordinates x_0 and y_0 define the escape location of the image rays at the acquisition surface S_a and t_0 is their one-way traveltimes. The curved datum level in depth then corresponds to a curve of some constant time t_0 that represents the image wavefront. Given the same focusing functions at the acquisition surface, the focusing position defined in the time-imaging domain (x_0, y_0, t_0) can be translated to its corresponding Cartesian position through the same mapping. Equipped with these results, we can proceed with making use of efficient time-domain techniques to solve the Marchenko equations and obtain focusing functions associated with some specified position in the time-imaging domain.

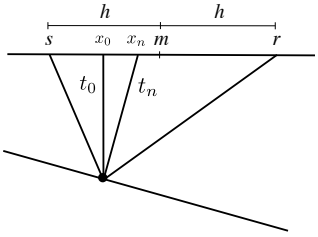

Figure 2: A schematic summarizing the concept behind prestack time migration after Fowler (1997).

SLOPE-BASED TIME-DOMAIN PROCESSING

The process of time-domain imaging can be conceptually summarized as shown in Figure 2 (Fowler, 1997). The recorded CMP data (m, h, t) is first migrated to zero-offset (x_n, t_n) through a combination of normal and dip moveouts. Poststack time migration subsequently maps the result to (x_0, t_0) for a correct position of subsurface reflecting point. The entire process constitutes the time-imaging routine and is equivalent to prestack time migration process. Fomel (2007) showed that under the regular assumptions of hyperbolic traveltime and straight-ray

geometry of time imaging, prestack time migration (mapping) can be done with local event slopes as follows:

$$t_0^2 = \frac{t p_h \left[(t - h p_h)^2 - h^2 p_m^2\right]^2}{4(t - h p_h)^2 \left[t p_h + h(p_m^2 - p_h^2)\right]} , \tag{5}$$

$$x_0 = m - \frac{h t p_y}{t p_h + h(p_m^2 - p_h^2)} , \tag{6}$$

where t is the two-way reflection traveltime. $p_m = \partial t / \partial m$ and $p_h = \partial t / \partial h$ are estimated local event slopes from the CMP gathers in the midpoint and half-offset directions, respectively.

From Figure 2, we can observe that the traveltime of direct-wave Green's function from the same subsurface position is represented by the same value of t_0 in the time-imaging domain. Consequently, the desired traveltime of the direct-wave Green's function from that location is simply a contour of time t_0 of the one-way traveltime map (equation 5). Therefore, we can summarize the steps to obtain slope-based direct-wave Green's function and solve the Marchenko system as follows:

1. Given the CMP gathers, measure the slopes of primaries using methods such as plane-wave destruction (Fomel, 2002) and generate the traveltime $t_0(m, h, t)$ and distance $x_0(m, h, t)$ maps according to equations 5 and 6.
2. Remap the t_0 data according to the x_0 data to correctly position the traveltime across the midpoint coordinate and obtain $t_0(x_0, h, t)$.
3. Specify a desired focusing position in (x_0, t_0) and obtain the traveltime of the direct-wave Green's function from the corresponding contour of $t_0(x_0, h, t)$.
4. Simply convolve with a zero-phase wavelet to obtain the approximate direct-wave Green's function.
5. Use the time-reversed direct-wave Green's function as the initial focusing function and solve the constrained Marchenko system 3 (van der Neut et al., 2015).

EXAMPLES

In this section, we apply the proposed workflow to two cases of 1D and 2D layered media. The CMP gathers are generated with Kirchhoff modeling based on an accurate two-point ray-tracing scheme (Sripanich and Fomel, 2014).

1D model

We first consider a horizontally layered model shown in Figure 3a and look at the Green's function from (0, 1000) on the third reflector. The true Green's function from forward modeling is shown in Figure 4a overlain by the traveltime prediction (magenta line) of the direct wave using the proposed slope-based workflow. We use the prediction to generate the initial focusing function and solve the Marchenko system (equation 3). The result from the usual velocity-based workflow is shown in Figure 4b in comparison with that from the proposed slope-based method in Figure 4c. The results are comparable in quality indicating the validity of the proposed method.

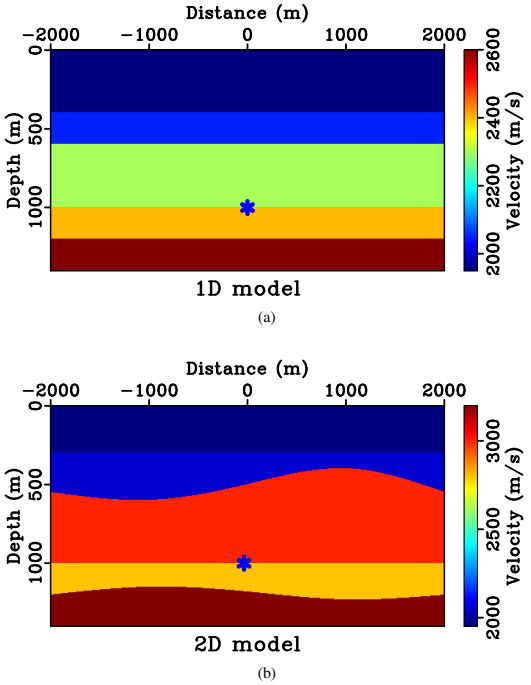

Figure 3: Synthetic models: (a) 1D with vertical image rays and (b) 2D with bending image rays used in our numerical experiments.

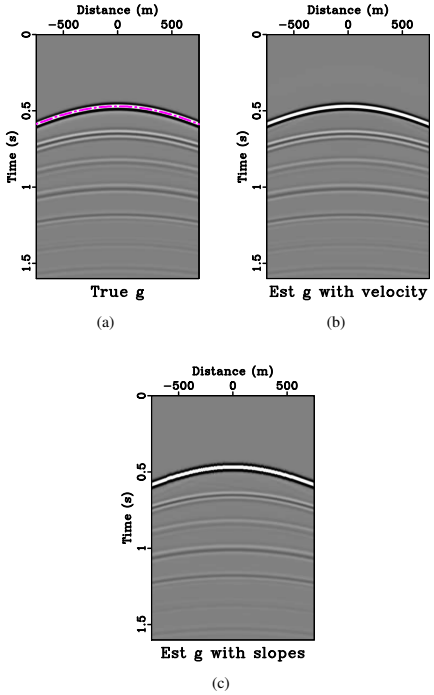

Figure 4: A comparison in a 1D model of the true Green's function (a) and estimated ones using the true velocity to generate initial focusing functions (b) and that from the proposed slope-based workflow (c). The dashed magenta line in (a) denotes the estimated traveltime of the direct wave using local slopes.

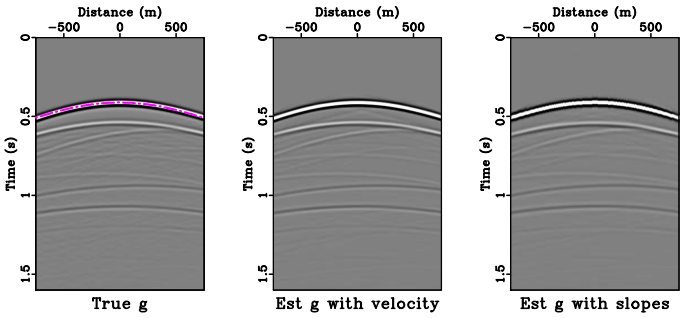

Figure 5: A comparison in a 2D model of the true Green's function (a) and estimated ones using the true velocity to generate initial focusing functions (b) and that from the proposed slope-based workflow (c). The dashed magenta line in (a) denotes the estimated traveltime of the direct wave using local slopes.

2D model

Next, we turn to a 2D layered model with lateral heterogeneity. In this example, the image rays are no longer vertical and the focusing positions in the time- and depth-imaging domains are related through the mapping defined by image rays. We consider the Green's function from (-35, 1000) on the third reflector because this is the position where the image ray originating from (0, 0) will pass through. We follow the same procedure as before and the comparison of Green's functions are shown in Figure 5. The results again are comparable in quality and similar conclusions can be drawn. We emphasize that the focusing position is defined in terms of (x_0, t_0) as opposed to (x, z) in the usual Marchenko workflow. To confirm that the specified focusing (x_0, t_0) translate to the Cartesian (x, z) according to the image ray mapping, we back propagate the computed focusing function and the result is shown in Figure 6. The dashed line is vertical, whereas the solid line is the image ray originating from (0, 0). We can observe that the response is now positioned along the image ray and is at the reflector we chose to compute our slope for the traveltime prediction in the first place.

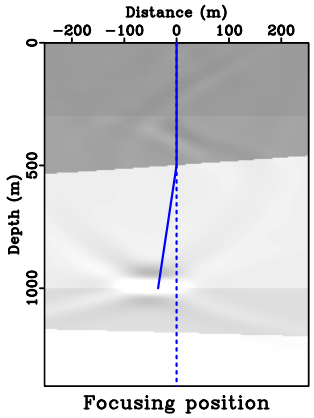

Figure 6: The focused response in the 2D model. Due to the specification of focusing position in the time-imaging domain (x_0, t_0), the focused position lies along the image ray (solid).

DISCUSSION AND CONCLUSION

In this paper, we first formulate the Marchenko system in the time-imaging domain defined by image rays. We show that the resulting Marchenko equations remain the same as in the previous case of a constant-depth datum level except that the integrations are now carried out along curved space boundaries of constant time. The prior knowledge of subsurface velocity is no longer needed and the Marchenko method can be accomplished by making use of local event slopes measured directly from CMP gathers. The focusing positions are now defined in terms of image-ray coordinates related to the surface location and vertical traveltime easily obtained from the data without any prior knowledge of the subsurface model.

We emphasize that we only make use of the slope-based workflow to obtain the traveltime of the direct-wave Green's function. The amplitude information is controlled by the choice of the convolving waveform. The coda of the resulting focusing functions and Green's functions from our scheme is therefore, scaled proportionately to this choice. Finding a dynamically appropriate waveform from slopes is a subject of future research. In a companion paper (Sripanich and Vasconcelos, 2018), we investigate another benefit from considering the Marchenko method in the time-imaging domain by analyzing the directionality of the focused responses with respect to the surface data aperture.

Finally, in our scheme, it is crucial that only the slopes of target primary reflection events are used for traveltime prediction. This can be done by prior interpretation of target reflections or by means of an expeditious multiple removal based on local slopes using simple velocity filtering (Cooke et al., 2009).

ACKNOWLEDGEMENT

We thank J. Brackenhoff, F. Broggini, S. Fomel, G. Meles, J. Thorbecke, and C. Urruticoechea for helpful discussions. This work is supported by the European Research Council (ERC) under the European Union's Seventh Framework Programme (FP/2007-2013) grant agreement number 320639 (iGEO).

REFERENCES

Berkhout, A. J., 1997, Pushing the limits of seismic imaging, Part I: Prestack migration in terms of double dynamic focusing: Geophysics, **62**, no. 3, 937–954.

Broggini, F., and R. Snieder, 2012, Connection of scattering principles: a visual and mathematical tour: European Journal of Physics, **33**, 593–613.

Broggini, F., R. Snieder, and K. Wapenaar, 2012, Focusing the wavefield inside an unknown 1D medium: Beyond seismic interferometry: Geophysics, **77**, no. 5, A25–A28.

Cameron, M. K., S. Fomel, and J. A. Sethian, 2007, Seismic velocity estimation from time migration: Inverse Problems, **23**, 1329–1369.

Cooke, D., A. Bóna, and B. Hansen, 2009, Simultaneous time imaging, velocity estimation and multiple suppression using local event slopes: Geophysics, **74**, no. 6, WCA65–WCA73.

Fomel, S., 2002, Application of plane-wave destruction filters: Geophysics, **67**, 1946–1960.

———, 2007, Velocity-independent time-domain seismic imaging using local event slopes: Geophysics, **72**, no. 3, S139–S147.

———, 2013, Wave-equation time migration: 83th Annual Meeting Expanded Abstracts, SEG, 3703–3708.

———, 2014, Recent advances in time-domain seismic imaging: 84th Annual Meeting Expanded Abstracts, SEG, 4400–4404.

Fowler, P., 1997, A comparative overview of prestack time migration methods: 67th Annual Meeting Expanded Abstracts, SEG, 1571–1574.

Frijlink, M., and K. Wapenaar, 2010, Reciprocity theorems for one-way wave fields in curvilinear coordinate systems: SIAM Journal of Imaging Sciences, **3**, no. 3, 390–415.

Hubral, P., 1977, Time migration—some ray theoretical aspects: Geophysical Prospecting, **25**, 738–745.

Sava, P., and S. Fomel, 2005, Riemannian wavefield extrapolation: Geophysics, **70**, no. 3, T45–T56.

Slob, E., K. Wapenaar, F. Broggini, and R. Snieder, 2014, Seismic reflector imaging using internal multiples with marchenko-type equations: Geophysics, **79**, no. 2, S63–S76.

Sripanich, Y., and S. Fomel, 2014, Two-point seismic ray tracing in layered media useing bending: 84th Annual Meeting Expanded Abstracts, SEG, 3371–3376.

———, 2018, Fast time-to-depth conversion and interval velocity estimation in the case of weak lateral variations: Geophysics, **83**, no. 3, S227–S235.

Sripanich, Y., and I. Vasconcelos, 2018, Effects of aperture on Marchenko focusing functions and their radiating directions: Presented at the 88th Annual Meeting Expanded Abstracts, SEG. (submitted).

Thorbecke, J., 1997, Common focus point technology: PhD thesis, Delft University of Technology.

Thorbecke, J., E. Slob, J. Brackenhoff, J. van der Neut, and K. Wapenaar, 2017, Implementation of the marchenko method: Geophysics, **82**, no. 6, WB29–WB45.

van der Neut, J., I. Vasconcelos, and K. Wapenaar, 2015, On green's function retrieval by iterative substitution of the coupled marchenko equations: Geophysical Journal International, **203**, 792–813.

Wapenaar, K., and J. Grimbergen, 1996, Reciprocity theorems for one-way wavefields: Geophysical Journal International, **127**, 169–177.

Wapenaar, K., J. Thorbecke, J. van der Neut, F. Broggini, E. Slob, and R. Snieder, 2014a, Green's function retrieval from reflection data, in absence of a receiver at the virtual source position: Journal of the Acoustical Society of America, **135**, no. 5, 2847–2861.

———, 2014b, Marchenko imaging: Geophysics, **79**, no. 3, WA39–WA57.

Wapenaar, K., J. Thorbecke, J. van der Neut, E. Slob, and R. Snieder, 2017, Review paper: Virtual sources and their responses, Part II: data-driven single-sided focusing: Geophysical Prospecting, **65**, no. 6, 1430–1451.

Yilmaz, O., 2001, Seismic data analysis, 2 ed.: SEG.